Smoothing effect for spatially distributed renewable resources and its impact on power grid robustness

Motoki Nagata,[1] Yoshito Hirata,[1,2] Naoya Fujiwara,[3] Gouhei Tanaka,[1,2,4] Hideyuki Suzuki,[5] and Kazuyuki Aihara[1,2,4]

[1]*Graduate School of Information Science and Technology, The University of Tokyo, Tokyo, Japan*

[2]*Institute of Industrial Science, The University of Tokyo, Tokyo, Japan*

[3]*Center for Spatial Information Science, The University of Tokyo, Chiba, Japan*

[4]*Graduate School of Engineering, The University of Tokyo, Tokyo, Japan*

[5]*Graduate School of Information Science and Technology, Osaka University, Osaka, Japan*

(Dated: January 20, 2017)

Abstract

In this paper, we show that spatial correlation of renewable energy outputs greatly influences the robustness of the power grids against large fluctuations of the effective power. First, we evaluate the spatial correlation among renewable energy outputs. We find that the spatial correlation of renewable energy outputs depends on the locations, while the influence of the spatial correlation of renewable energy outputs on power grids is not well known. Thus, second, by employing the topology of the power grid in eastern Japan, we analyze the robustness of the power grid with spatial correlation of renewable energy outputs. The analysis is performed by using a realistic differential-algebraic equations model. The results show that the spatial correlation of the energy resources strongly degrades the robustness of the power grid. Our results suggest that we should consider the spatial correlation of the renewable energy outputs when estimating the stability of power grids.

LEAD PARAGRAPH

The renewable energy resources, such as photovoltaics and wind powers, cause large power fluctuations that may result in blackouts. In order to avoid such blackouts, it is important to understand the influence of renewable energy resources on power grids' stability [1, 2]. The output powers of renewable energy resources, which depend on the weather conditions, can be spatially correlated if their locations are geographically close. However, few studies have addressed the effect of such spatially correlated energy generations on the power grid robustness. Here, we evaluate the spatial correlation among renewable energy outputs. We find that the spatial correlation of renewable energy outputs depends on the locations. Therefore, next we examine the influence of the spatial correlation of renewable energy outputs on power grids. We clarify that spatial correlation of renewable energy outputs makes power grids fragile. Our results indicate that one should take into account the spatial correlation of the renewable energy outputs when evaluating the stability of power grids.

I. INTRODUCTION

A lot of renewable energy resources are being incorporated into power networks for realizing low carbon societies. More and more renewable energy resources will be introduced in all over the world. For example, in Japan, the amount of photovoltaics (PV) introduction in 2030 is expected to be about ten times larger than that in 2012 [3]. The large amount of renewable energy resources, especially wind and solar powers which are connected to end users, can cause large power fluctuations that may result in blackouts. When analyzing the robustness of the power grids against large fluctuations of the effective power based on mathematical models, we cannot use linearization schemes in the presence of large power fluctuations, because the model behavior is far from a steady state. A method that enables to quantify the robustness of stable states against large fluctuations in differential equations was proposed in Ref. [4], where the robustness is measured by the volume of the basins of attraction of the stable states. This method was used to investigate the relation between the network topology and the robustness of power grids against large fluctuations [5].

In the studies of power grids in the physics community, the Kuramoto-like phase oscillator model, which qualitatively corresponds to the swing equation in the electrical engineering community, has often been used in order to clarify various properties of power grids [5–12]. Although the model is simple and mathematically tractable, the model has drawbacks in the sense that it does not take into account some factors which play important roles in the stability of power grids, particularly fluctuations in the voltage amplitude and the adjustment of reactive power in substations [2]. In order to study the effects of these factors on the stability of the power grids with relatively simple models, a new mathematical model governed by differential-algebraic equations was proposed [1]. In this model, the properties of generators are described using the swing equations [6–12], while the properties of substations are determined with the power flow calculation. Differential-algebraic equations models are also standard in the study of power grids. We note that there are some differential equations models that include the voltage dynamics by considering machines' electrodynamical behavior [13, 14]. The recent application in a more physical context is explained in Ref. [15]. We proposed a new method to analyze the robustness against large fluctuations of the power grid system governed by this differential-algebraic equations model in Ref. [2].

Among various aspects of renewable energy outputs intensively studied so far [16], the smoothing effect is notable [17, 18]. The smoothing effect indicates that the fluctuations in the total amount of renewable energy outputs are smaller than the sum of fluctuations in the individual renewable energy outputs because the individual fluctuations are balanced out. Although the smoothing effect seems to enhance the robustness of the power grid, we need to take into account the spatial correlation of the weather conditions [19, 20], which may destabilize the system locally. We evaluate the spatial correlation among renewable energy outputs. We find that the spatial correlation of renewable energy outputs depends on the locations. Therefore, it is significant to understand the relation between the spatial correlation and the robustness of power grids.

In this study, we analyze the relation between the smoothing effect and the robustness of power grids by extending the method proposed in Ref. [2]. We show that the spatial correlation, and thus the lack of the smoothing effect, makes power grids more fragile. Our analysis may contribute to the precursor detection of the blackout by using the method of dynamical network marker [21].

There are three types of stability in the power system: voltage stability, frequency stability, and phase angle stability [22]. This research focuses on voltage stability among them. Stability analysis of the power system is mainly separated into steady state stability analysis and transient stability analysis [22]. The steady state stability analysis is to analyze the stability against small fluctuations, and the transient stability analysis is the analysis of the stability against large fluctuations. In this study, we analyze the stability against large fluctuation, i.e., the transient stability analysis. Other methods about the transient stability analysis are described in Refs. [23, 24]. Moreover, there is another stability called structural stability, which is discussed in Ref. [25].

This paper is organized as follows. First, in Sec. II, we give a brief overview of the model of the power grids. Then, in Sec. III, we evaluate the spatial correlation among renewable energy outputs. Section IV is devoted to clarifying the relation between the smoothing effect and the robustness of power grids using the real power grid topology in eastern Japan. Finally, in Sec. V, we conclude this paper.

II. A DYNAMICAL MODEL OF POWER GRIDS AND A ROBUSTNESS MEASURE

A. Differential-algebraic equations model

We introduce the differential-algebraic equations model for power grids proposed by Sakaguchi and Matsuo [1]. Detailed analysis was given in Ref. [2].

Power grids consist of generators, substations, and end-users including buildings, factories, and houses. Recently, an increasing number of solar panels are connected to the end-users. The transmitted energy from generators to substations is equal to the difference between the energy consumed by end-users and the output energy of the solar panels. Therefore, large fluctuations in powers generated by the solar panels can cause large fluctuations of the transmitted energy from generators to substations. The voltages for the transmission lines between generators and substations are very high (500 kV or 275 kV in Japan). On the other hand, the voltages for the transmission lines between substations and end-users are relatively low (66 kV or 6.6 kV in Japan). Since the voltages are converted from high values to low values at substations, substations can be seen as substations from the high-voltage power grid. In this study, we focus on the parts with high-voltage transmission lines, i.e., generators and substations. The numbers of generators, substations, and branching points are denoted by N_g, N_l, and N_b, respectively, and the total number of generators and substations by $N_r \equiv N_g + N_l$.

Power grids are regarded as complex networks consisting of nodes which correspond to generators, substations, and branching points. We denote the voltage of node j by $V_j = |V_j| \exp(\mathrm{i}\theta_j)$ for $j = 1, \ldots, N_r$, where $|V_j|$ and θ_j are the amplitude and the phase of the voltage, respectively. Complex numbers are useful to represent the behavior of alternate-current voltages. The resistance is much smaller than the reactance in the transmission lines, and therefore, we can consider a power network where the resistance is neglected, i.e., a lossless network. We use the Kron's reduction in the same way as Refs. [2, 26, 27] and denote the reduced susceptance between node j and node k by B_{jk}.

We regard the generators as phase oscillators. We denote the difference between the phase θ_j and the phase advance by the standard frequency Ω by $\phi_j \equiv \theta_j - \Omega t$. This standard frequency Ω is $2\pi \times 60$ s^{-1} in the United States and western Japan, and $2\pi \times 50$ s^{-1} in Europe and eastern Japan. The behavior of each generator is described as follows [6]:

$$M_j \ddot{\phi}_j + D_j \dot{\phi}_j = P_j^m - \sum_{k=1}^{N_r} |V_j||V_k| B_{jk} \sin(\phi_j - \phi_k), \tag{1}$$

where M_j is the inertial coefficient, D_j is the damping coefficient, and P_j^m is the mechanical input energy. Equation (1) is called the 'swing equation' and derived from the energy conservation law. We adopt the local feedback control as follows [1]:

$$\dot{P}_j^m = -K_j \dot{\phi}_j, \tag{2}$$

where K_j corresponds to the inverse of the time constant. The impact of feedback control (cf. equation (2)) on transient stability was recently analyzed in Ref. [28].

The behavior of each substation is written as follows:

$$P_j = \sum_{k=1}^{N_r} |V_j||V_k| B_{jk} \sin(\phi_k - \phi_j), \tag{3}$$

$$Q_j = \sum_{k=1}^{N_r} |V_j||V_k| B_{jk} \cos(\phi_k - \phi_j), \tag{4}$$

where P_j and Q_j are the consumed effective energy and the consumed reactive energy in substations, respectively. If the reactive energy is supplied in substations, Q_j is negative. Equations (3) and (4) are derived from Kirchhoff's and Ohm's laws. Each iteration of our numerical simulation consists of two steps: First, we used the fourth-order Runge–Kutta method to simulate the generators' Eq. (1). We set the time step to 0.005. Second, we used Newton's method for the substations' Eqs. (3) and (4). We repeated this iteration for sufficiently many times until a convergence is reached. We use the values of $|V_j|$ and ϕ_j at substation nodes in the previous step to obtain ϕ_j of generator node j when simulating the generators' Eq. (1). On the other hand, we use the value of ϕ_j at generator j in the current step to obtain P_j and Q_j of substation node j when solving the substations' Eqs. (3) and (4).

B. Robustness evaluation

We set the effective power in substations stochastically, while we keep the reactive power in substations constant. By simulating the generators' Eq. (1) and the substations' Eqs. (3) and (4), we judge whether the solution for Eqs. (3) and (4) exists. The case where the solution does not exist corresponds to the power shortage, because this absence means that the power grid cannot realize such a power flow. In this case, the voltage collapse occurs. It should be noted that real power grids have to operate satisfying physical constraints of the components such as generators, substations, and transmission lines, which can be violated earlier than the voltage collapse we consider here. However, we employ this simple model in order to observe the qualitative behavior of power grids.

We calculate the probability that the solution exists and define the stability rate as this probability. We evaluate the robustness based on the stability rate. In this paper, we study the relation between the spatial correlation and the robustness of power grids.

III. SPATIAL CORRELATION OF RENEWABLE ENERGY OUTPUTS

A. Smoothing effect

The smoothing effect [17, 18] means that the fluctuations in the total of renewable energy outputs are smaller than the sum of the fluctuations in the individual outputs. This is a remarkable aspect of renewable energy outputs.

We evaluate the spatial correlation among renewable energy outputs in order to clarify how much the smoothing effect holds; the larger the smoothing effect is, the lower the spatial correlation is.

B. Spatial correlation of renewable energy output data

Let us denote the output data of renewable energy in node i by $x_i(t)$ where t is the index of the sample $(t = 1, 2, \ldots, T)$ and the vector of the data by $\mathbf{x}_i = \{x_i(t)\}_{t=1}^{T}$. We evaluate the spatial correlation by using the Pearson correlation coefficient (PCC) between each two nodes. The PCC between nodes i and j is defined as follows:

$$\mathrm{PCC}_{ij} \overset{\mathrm{def}}{=} \frac{Cov(\mathbf{x}_i, \mathbf{x}_j)}{\sqrt{V(\mathbf{x}_i)V(\mathbf{x}_j))}}, \qquad (5)$$

where $Cov(\mathbf{x}, \mathbf{y})$ and $V(\mathbf{x})$ are given by

$$Cov(\mathbf{x}, \mathbf{y}) = \frac{1}{T-1} \sum_{t=1}^{T} \Big(x(t) - \frac{1}{T} \sum_{\tau=1}^{T} x(\tau) \Big) \Big(y(t) - \frac{1}{T} \sum_{\tau=1}^{T} y(\tau) \Big), \qquad (6)$$

$$V(\mathbf{x}) = \frac{1}{\text{[illegible]}} \sum^{T} \Big(x(t) - \frac{1}{\text{[illegible]}} \sum^{T} x(\tau) \Big)^2 \qquad (7)$$

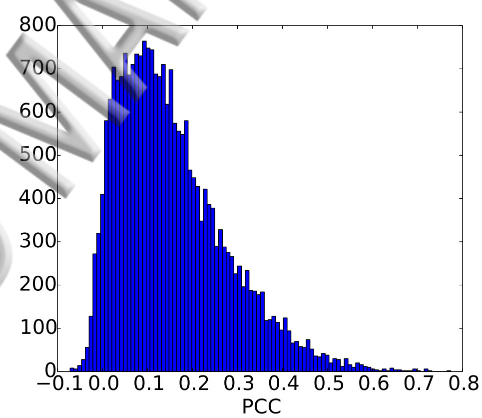

FIG. 1. The histogram of the PCC of wind power obtained from cubed wind speed data at 154 measurement points in Japan. The horizontal axis represents the PCC between each two nodes. The step size is set at 10 minutes. The vertical axis represents the counts.

We evaluated the PCC for wind power obtained from cubed wind speed data at 154 measurement points in Japan (Fig. 1) and that for solar radiation data at 7 measurement points in the Kanto area, Japan (Fig. 2) for different size of the time window. The time period for wind speed data and that for solar radiation data are between January 1, 2010 and December 31, 2012 and between January 1, 2011 and December 31, 2011, respectively.

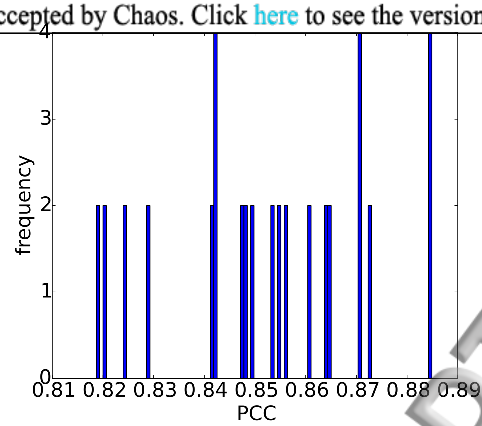

FIG. 2. The histogram of the PCC of solar radiation data at 7 measurement points in Japan. The horizontal axis represents the PCC between each two nodes. The step size is 1 minute. The vertical axis represents the counts.

The both figures show that the spatial correlation of renewable energy outputs depends on the locations. Therefore, it is significant to understand the relation between the spatial correlation and the robustness of power grids.

IV. IMPACT OF SMOOTHING EFFECT ON ROBUSTNESS OF THE POWER GRIDS

We simulated the differential-algebraic equations model for the power grid in eastern Japan by taking into account the smoothing effect found in the previous section. The correlated noise with various PCCs was generated by the method proposed in Ref. [29].

A. Eastern Japan power grid

Figure 3 shows the topology of the high voltage power grid in eastern Japan. It was derived from the reports released by Tokyo Electric Power Company Inc. [30] and Tohoku Electric Power Company Inc. [31]. The figure was produced with the graph visualization software Gephi [32]. This power grid consists of $N_g = 53$, $N_l = 126$, and $N_b = 69$ nodes. The number of nodes corresponding to generators and substations is $N_r = N_g + N_l = 179$ and the total number of nodes in the power grid is $N = 248$. In addition, we set the parameter values to $M_j = 1$, $D_j = 1$, $K_j = 30$, $P_j^m(0) = 1$, and $Q_j = 0$ as adopted in Ref. [2]. The

FIG. 3. (Color online) The topology of the high voltage power grid in eastern Japan that we derived. The red circles represent generators, the green circles represent substations, and the small gray circles represent branching points.

admittance matrix for the links was set as follows:

$$B_{jk} = \begin{cases} 10, & \text{if node } j \text{ and node } k \text{ are connected,} \\ 0, & \text{otherwise.} \end{cases} \tag{8}$$

Because the real-world parameters of the power grids in Japan have not been published, we set the parameters heuristically by following the previous research of Ref. [5]. It is our future work to carry out the same analysis with real data of other countries [33].

B. Results

We gave a fluctuation of the consumed effective power in each substation, i.e., P_j. We set P_j stochastically, update it at discrete time points, and keep it constant in between. Using the method of Ref. [29], the distribution for each of the 126 effective powers was adjusted to the distribution of wind power obtained from cubed wind speed data at one of 154

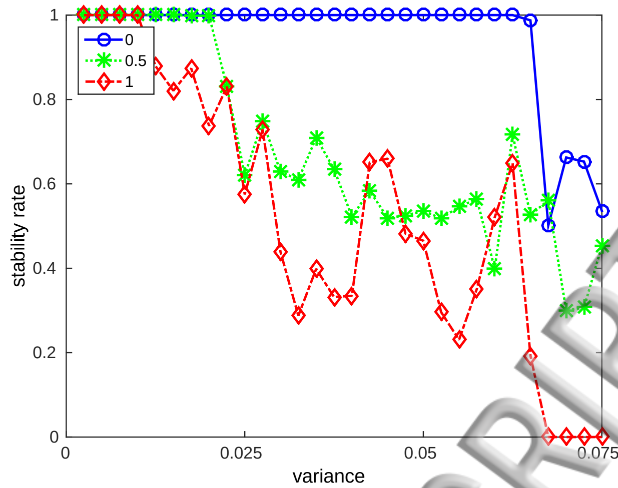

FIG. 4. The relation between the variance of fluctuations and the stability rate. The horizontal axis represents the variance of the fluctuations in each node. The vertical axis represents the stability rate. The open circles with the solid line show the result when the PCC of the fluctuations in each two nodes is 0. The asterisks with the dashed line correspond to the result when the PCC of the fluctuations in each two nodes is set at 0.5. The rhombi with the dash-dotted line correspond to the result when the PCC of the fluctuations in each two nodes is set at 1.

measurement points in Japan mentioned in Sec. III B, and the PCC between every pair of the effective powers was set to a value we specify in each of numerical simulations. The time resolution of the simulated noise is the same as the time step of the numerical simulation, which is 0.005. The mean of the effective power P_j was fixed at 0.45. In addition, we varied the variance of P_j from 0 to 0.15. For simplicity, we assumed that the mean and the variance of the fluctuations are identical for all nodes and the PCC of each two nodes is the same. Figure 4 shows the relation between the variance of fluctuations and the stability rate. The open circles with the solid line indicate the result when the PCC of the fluctuations in each two nodes is 0. The asterisks with the dashed line indicate the result when the PCCs are set at 0.5. The rhombi with the dash-dotted line indicate the result when the PCCs are set at 1. Clearly, the power grids become more unstable when the fluctuations are more correlated. Figure 5 shows the relation between the PCCs and the stability rate. The horizontal axis represents the PCC of the fluctuations in each two nodes. The vertical axis represents the stability rate. Especially in the area with a lower PCC, the larger the PCC is, the more unstable the power grid is. This tendency indicates that the smoothing effect makes the

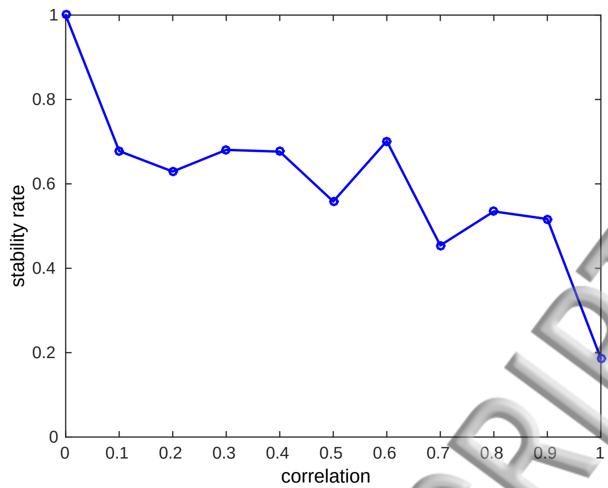

FIG. 5. The relation between the PCC of fluctuations and the stability rate. The horizontal axis represents the PCC of the fluctuations in each two nodes. The vertical axis represents the stability rate.

PCC closer to zero and stabilizes the power grid.

V. DISCUSSIONS

It may be wondered whether correlation coefficients of the 10 minute resolution obtained in Figures 1 and 2 are not realistic for the simulations we conducted later. However, we observed, using a dataset of Ref. [34], that the value of the correlation coefficient between wind powers at two neighboring points increases when we apply the moving average with a wider time window (Fig. 6). Therefore, the correlation coefficients of the 10 minute resolution can be regarded as an upper bound for the correlation coefficients for the finer time resolution. Thus, the simulations conducted in Figs. 4 and 5 can be considered as the severest case we could imagine.

It may be also guessed that very large fluctuations can be handled if the grid operators are prepared. This is true when we can predict the fluctuations perfectly, such as the solar eclipse. However, we usually cannot predict the renewable energy outputs perfectly [35]. Therefore, the large amount of renewable energy resources can cause large power fluctuations that may result in blackouts.

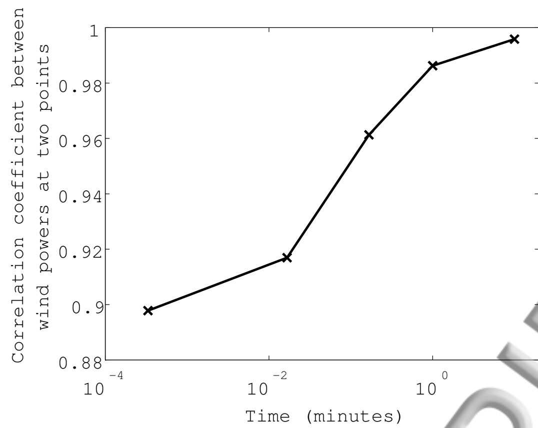

FIG. 6. The relation between the time scales of moving average and the correlation coefficient between wind powers at two points. The horizontal axis represents the time scales of moving average. The vertical axis represents the correlation coefficient between wind powers at two points.

VI. CONCLUSIONS

We have analyzed the relation between the smoothing effect and the robustness of power grids by using the mathematical model governed by differential-algebraic equations proposed in Ref. [1] and the real topology of the power grid in eastern Japan. We have clarified that the smoothing effect facilitates the robustness of the power grid. In other words, the spatial correlation of the renewable energy outputs degrades the robustness of the power grid, which is an important factor for studying the introduction of the renewable energy.

ACKNOWLEDGMENTS

We thank the Japan Meteorological Agency for providing the wind and solar irradiation datasets used in this study. This research was supported by Core Research for Evolutional Science and Technology (CREST), Japan Science and Technology Agency (JST).

[1] H. Sakaguchi and T. Matsuo, J. Physical Soc. Japan **81**, 074005 (2012).

[2] M. Nagata, N. Fujiwara, G. Tanaka, H. Suzuki, E. Kohda, and K. Aihara, Eur. Phys. J. Spec. Top. **223**, 2549 (2014).

[3] `http://www.jema-net.or.jp/Japanese/res/solar/mokuhyo.html`.

[4] P. J. Menck, J. Heitzig, N. Marwan, and J. Kurths, Nat. Phys. **9**, 89 (2013).

[5] P. J. Menck, J. Heitzig, N. Marwan, J. Kurths, and H. J. Schellnhuber, Nat. Commun. **5**, 1 (2014).

[6] G. Filatrella, A. H. Nielsen, and N. F. Pedersen, Eur. Phys. J. B **61**, 485 (2008).

[7] L. Buzna, S. Lozano, and A. Díaz-Guilera, Phys. Rev. E **80**, 066120 (2009).

[8] S. Lozano, L. Buzna, and A. Díaz-Guilera, Eur. Phys. J. B **85**, 231 (2012).

[9] M. Rohden, A. Sorge, M. Timme, and D. Witthaut, Phys. Rev. Lett. **109**, 064101 (2012).

[10] D. Witthaut and M. Timme, New J. Phys. **14**, 083036 (2012).

[11] F. Dörfler and F. Bullo, SIAM J. Control Optim. **50**, 1616 (2012).

[12] M. Nagata, I. Nishikawa, N. Fujiwara, G. Tanaka, H. Suzuki, and K. Aihara, in *Proceedings of 2013 International Symposium on Nonlinear Theory and its Application* (2013) pp. 69–72.

[13] J. Machowski, J. Bialek, and D. J. Bumby, *Power System Dynamics: Stability and Control, 2nd Edition* (WILEY, 2008).

[14] K. Schmietendorf, J. Peinke, R. Friedrich, and O. Kamps, The European Physical Journal Special Topics **223**, 2577 (2014).

[15] A. Gajduk, M. Todorovski, J. Kurths, and L. Kocarev, New Journal of Physics **16**, 115011 (2014).

[16] M. Lei, L. Shiyan, J. Chuanwen, L. Hongling, and Z. Yan, Renew. Sust. Energ. Rev. **13**, 915 (2009).

[17] H. Nagoya, S. Komami, and K. Ogimoto, IEEJ Transactions on Electronics, Information and Systems (in Japanese) **131**, 1688 (2011).

[18] H. Nagoya, M. Hosokawa, M. Ishimaru, S. Komami, and K. Ogimoto, IEEJ Transactions on Electrical and Electronic Engineering B (in Japanese) **133** (2013).

[19] P. Milan, M. Wächter, and J. Peinke, Phys. Rev. Lett. **110**, 138701 (2013).

[20] P. G. Lind, I. Herráez, M. Wächter, and J. Peinke, Energies **7**, 8279 (2014).

[21] L. Chen, R. Liu, Z.-P. Liu, M. Li, and K. Aihara, Scientific Reports **2** (2012).

[22] J. D. Hamilton, *Time Series Analysis* (Princeton Univ Pr, 1994).

[23] F. Hellmann, P. Schultz, C. Grabow, J. Heitzig, and J. Kurths, Scientific Reports **6** (2016).

[24] H.-D. Chiang, F. Wu, and P. Varaiya, IEEE Transactions on Circuits and Systems **34**, 160 (1987).

[25] D. Witthaut, M. Rohden, X. Zhang, S. Hallerberg, and M. Timme, Phys. Rev. Lett. **116**, 138701 (2016).

[26] P. Kundur, *Power System Stability and Control* (McGraw-Hill, Inc., New York, 1994).

[27] J. Machowski, J. Bialek, and D. Bumby, *Power System Dynamics: Stability and Control* (John Wiley and Sons, Inc., Chichester, UK, 2008).

[28] B. Schäfer, M. Matthiae, M. Timme, and D. Witthaut, New Journal of Physics **17**, 015002 (2015).

[29] T. Hiratsuka, K. Nozaki, M. Kato, and Y. Hirata, Renewable Energy and Power Quality Journal **1**, 105 (2013).

[30] http://www.tepco.co.jp/ir/tool/annual/index-j.html.

[31] http://www.tohoku-epco.co.jp/ir/report/annual_report/index.html.

[32] https://gephi.org/.

[33] http://wiki.openmod-initiative.org/wiki/Transmission_network_datasets.

[34] Y. Hirata, D. P. Mandic, H. Suzuki, and K. Aihara, Philosophical Transactions of the Royal Society of London A: Mathematical, Physical and Engineering Sciences **366**, 591 (2008).

[35] Y. Hirata, K. Aihara, and H. Suzuki, The European Physical Journal Special Topics **223**, 2451 (2014).

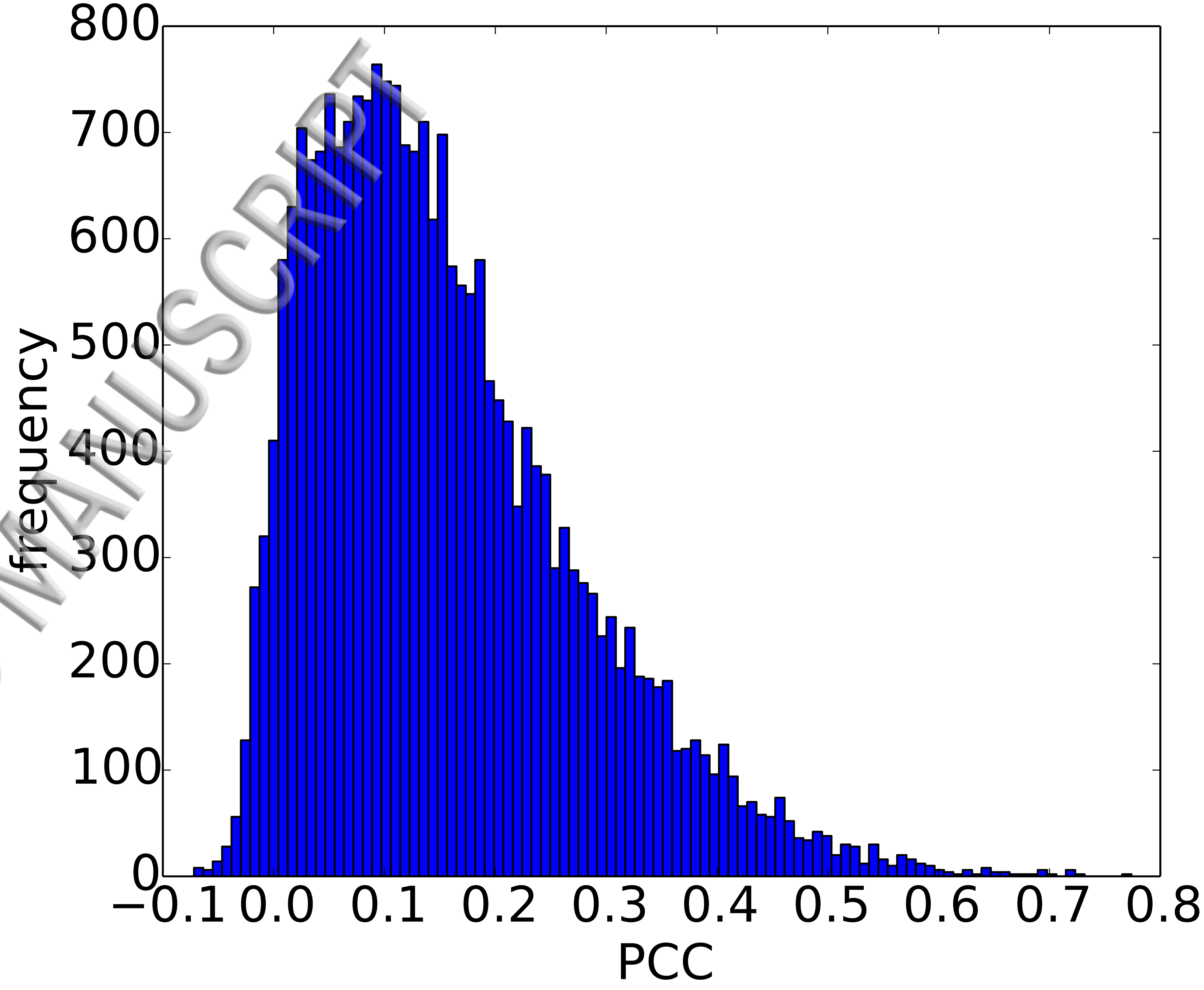

frequency
PCC
0
100
200
300
400
500
600
700
800
−0.1
0.0
0.1
0.2
0.3
0.4
0.5
0.6
0.7
0.8

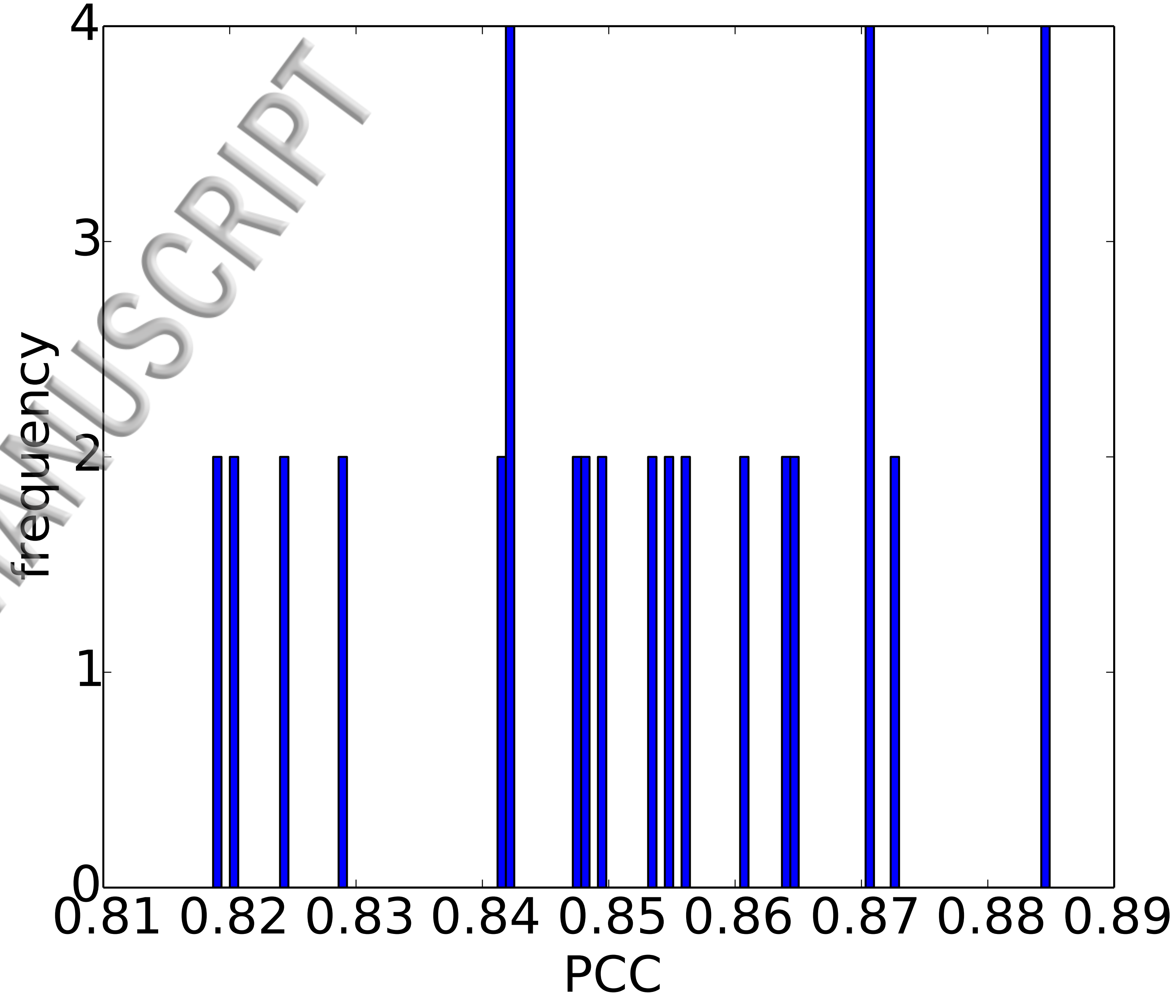
4
3
2
1
0
frequency
0.81 0.82 0.83 0.84 0.85 0.86 0.87 0.88 0.89
PCC

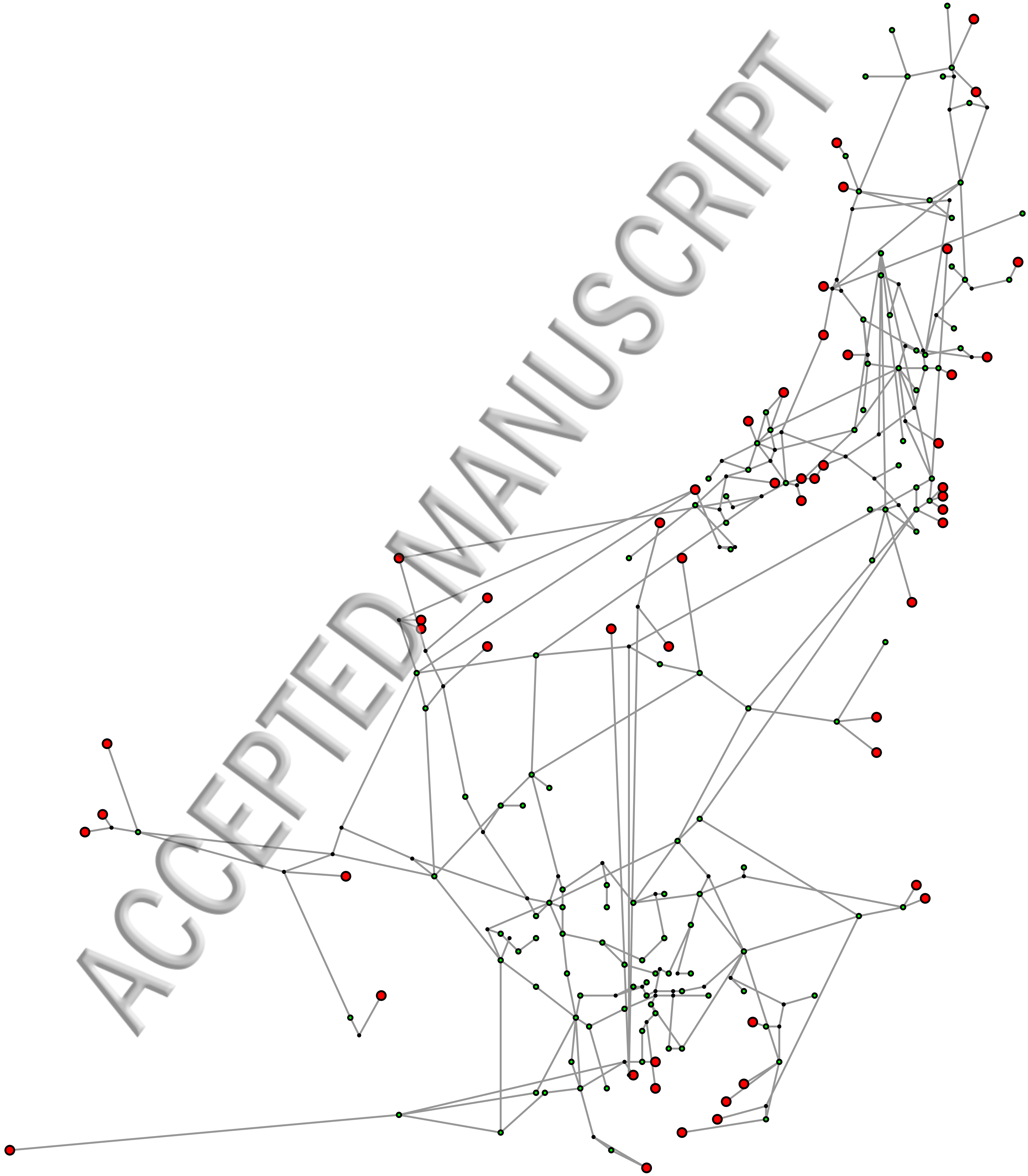

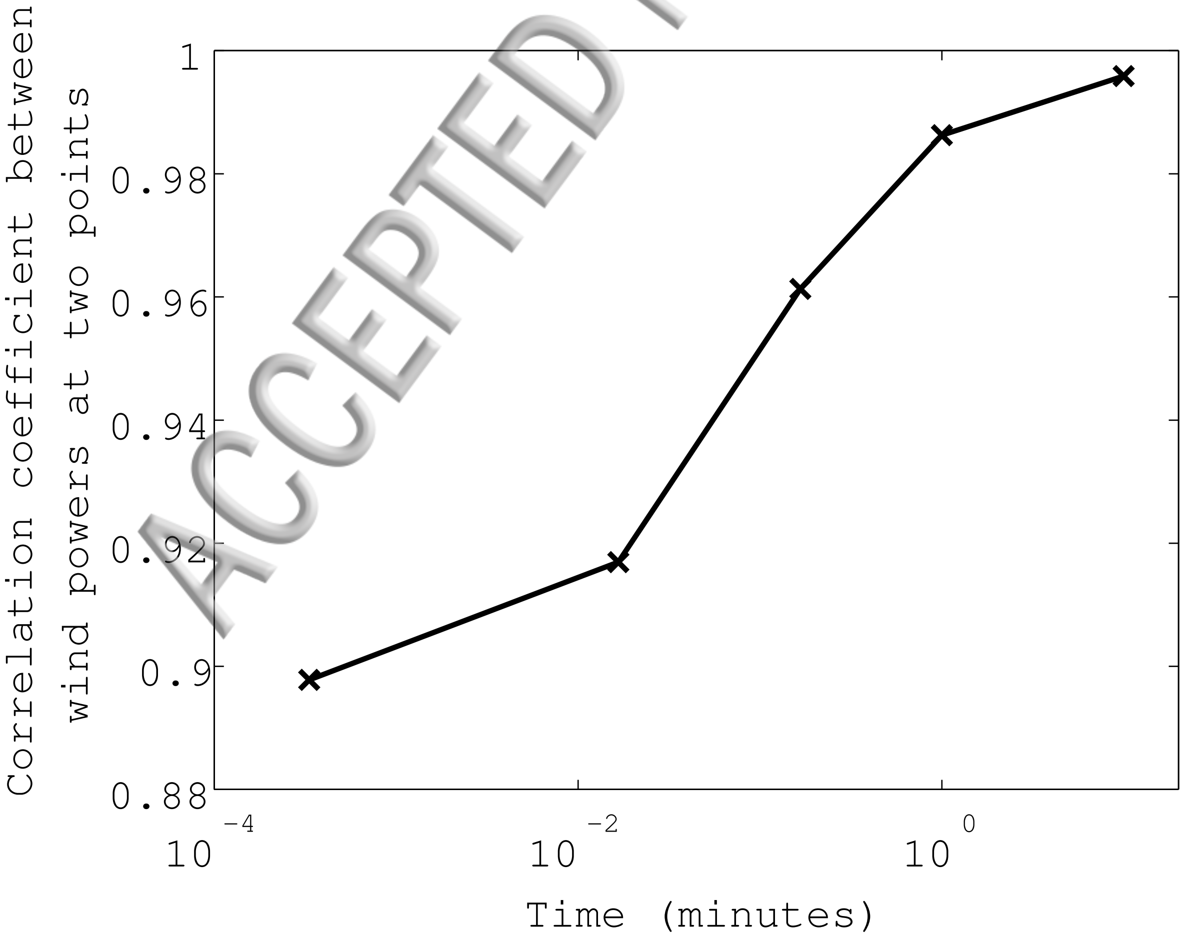
Correlation coefficient between
wind powers at two points
1
0.98
0.96
0.94
0.92
0.9
0.88
10^{-4}
10^{-2}
10^{0}
Time (minutes)